nature cell biology

# Isolated nuclei adapt to force and reveal a mechanotransduction pathway in the nucleus

Christophe Guilluy[1], Lukas D. Osborne[2], Laurianne Van Landeghem[1], Lisa Sharek[1], Richard Superfine[2], Rafael Garcia-Mata[1] and Keith Burridge[1,3,4]

**Mechanical forces influence many aspects of cell behaviour. Forces are detected and transduced into biochemical signals by force-bearing molecular elements located at the cell surface, in adhesion complexes or in cytoskeletal structures[1]. The nucleus is physically connected to the cell surface through the cytoskeleton and the linker of nucleoskeleton and cytoskeleton (LINC) complex, allowing rapid mechanical stress transmission from adhesions to the nucleus[2]. Whereas it has been demonstrated that nuclei experience force[3], the direct effect of force on the nucleus is not known. Here we show that isolated nuclei are able to respond to force by adjusting their stiffness to resist the applied tension. Using magnetic tweezers, we found that applying force on nesprin-1 triggers nuclear stiffening that does not involve chromatin or nuclear actin, but requires an intact nuclear lamina and emerin, a protein of the inner nuclear membrane. Emerin becomes tyrosine phosphorylated in response to force and mediates the nuclear mechanical response to tension. Our results demonstrate that mechanotransduction is not restricted to cell surface receptors and adhesions but can occur in the nucleus.**

To mimic the transmission of mechanical stress from the cytoskeleton to the nucleus, we applied force directly on isolated nuclei through the LINC complex component nesprin-1 (Fig. 1a). We used magnetic tweezers to stimulate magnetic beads coated with anti-nesprin-1 antibody and we measured bead displacements due to a known force induced by a magnetic field. Application of successive pulses of constant force triggered an increase in nuclear stiffness, resulting in decreased bead displacement (Fig. 1b and Supplementary Figs 1a and 2). The relative bead displacement was calculated by normalizing the displacement for pulses 2, 3, 4, 5 and 6 to that observed during the first pulse. The decrease in bead displacement was significant after the third pulse (Fig. 1c) and reached a maximum of 35% after the sixth pulse (Fig. 1c). A similar decrease in bead displacement was observed when we stimulated nuclei isolated from endothelial cells or fibroblasts with pulses of force (Fig. 1d), whereas no change in bead displacement was observed when beads were coated with poly-L-lysine (Fig. 1c) or when pulses of force were applied to nuclear pores using beads coated with anti-Nup358 antibody (Fig. 1e). These results show that applying tension on the LINC complex triggers a mechanotransduction pathway that adjusts the mechanical properties of the nucleus. We next investigated the molecular events that mediate this nuclear response to force.

The application of force on integrins induces a local stiffening response[4,5], also called reinforcement[6], that involves remodelling of the actin cytoskeleton and that requires the RhoA pathway[5,7]. Interestingly, both actin and RhoA have been reported to localize to the nucleus[8,9]. To determine the effect of force on nuclear RhoA activity, we used a permanent magnet to apply constant force on beads coated with anti-nesprin-1 antibody. We observed that force on nesprin-1 activates RhoA in isolated nuclei (Supplementary Fig. 3b); however, pharmacological inhibition of Rho or Rho-associated kinase (ROCK), respectively with C3 transferase or Y-27632, did not prevent nuclear stiffening in response to force (Fig. 2a). Consistent with this, we found that treatment of nuclei with agents that disrupt actin filaments (latrunculin A or cytochalasin D) did not affect stiffening of isolated nuclei in response to force (Fig. 2b). These results indicate that distinct molecular mechanisms regulate the mechanical adaptation to force that occurs at the cell surface and in the nucleus.

Both the nucleoskeleton and chromatin contribute to the mechanical properties of the nucleus[10,11]. To determine whether a change in the mechanical properties of DNA contributes to the nuclear stiffening in response to force, we used nuclei isolated from cells treated with trichostatin A, a histone deacetylase inhibitor that causes DNA decondensation. Treatment with trichostatin A did not prevent force-induced nuclear stiffening (Fig. 2b), although

[1]Department of Cell Biology and Physiology, University of North Carolina at Chapel Hill, Chapel Hill, North Carolina 27599, USA. [2]Department of Physics and Astronomy, University of North Carolina at Chapel Hill, Chapel Hill, North Carolina 27599, USA. [3]Lineberger Comprehensive Cancer Center, and UNC McAllister Heart Institute, University of North Carolina, Chapel Hill, North Carolina 27599, USA.
[4]Correspondence should be addressed to K.B. (e-mail: Keith_Burridge@med.unc.edu)

Received 3 August 2013; accepted 3 February 2014; published online XX Month XXXX; DOI: 10.1038/ncb2927

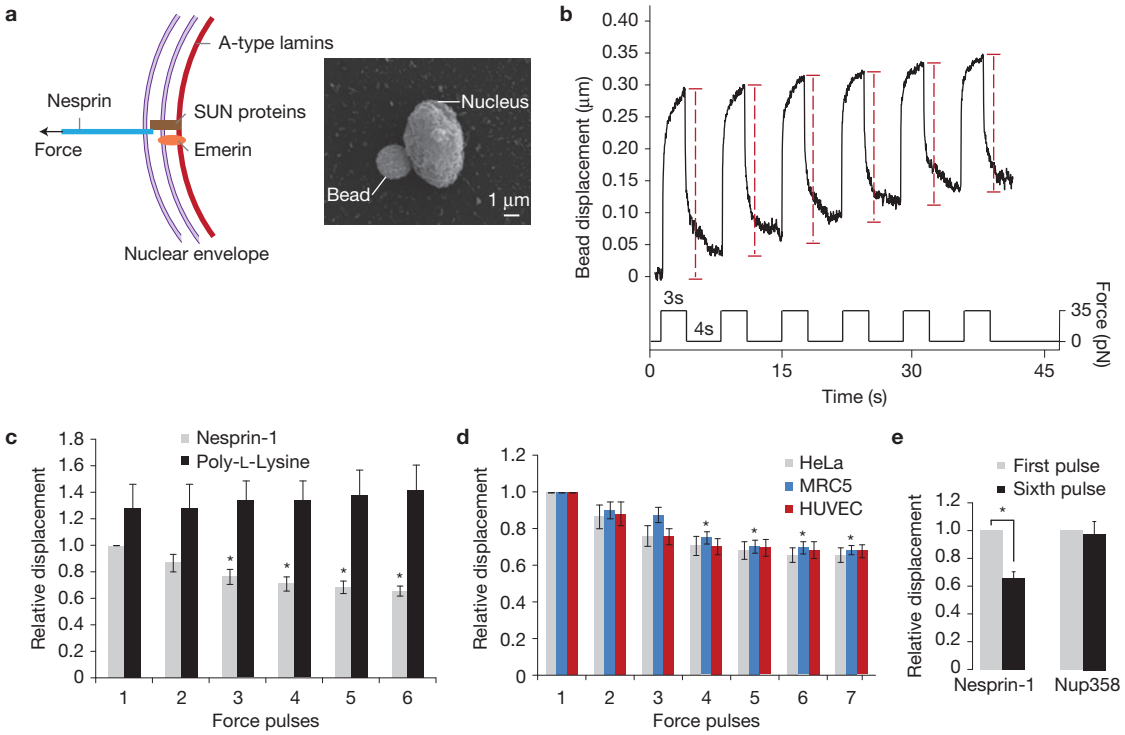


**Figure 1** Isolated nuclei stiffen in response to force applied on nesprin-1. (**a**) Left, diagram of the LINC complex showing where tensional forces were applied to mimic the transmission of mechanical stress from the cytoskeleton to the nucleus. Right, scanning electron micrograph of a magnetic bead attached to a nucleus isolated from a HeLa cell. Result is representative from 6 independent experiments. (**b**) Typical displacement of a 2.8 μm bead coated with anti-nesprin-1 antibody bound to an isolated nucleus during force pulse application. Stiffening is indicated by decreased displacement during later pulses. (**c**) Change in bead displacement during 6 force pulses applied to beads coated with anti nesprin-1 antibody ($n=18$ beads) or poly-L-lysine ($n=14$ beads) and bound to nuclei isolated from HeLa cells. Displacements were calculated relative to the first pulse of force applied to beads coated with anti-nesprin-1 (error bars represent s.e.m., $^*P<0.05$, data were collected from 3 independent experiments and analysed by one-way analysis of variance (ANOVA)). (**d**) Change in bead displacement during 7 force pulses applied to beads coated with anti-nesprin-1 bound to nuclei isolated from HeLa cells ($n=18$ beads), MRC5 cells ($n=21$ beads) or HUVECs ($n=15$ beads). Displacements were calculated relative to the first pulse of force (error bars represent s.e.m., $^*P<0.05$, data were collected from 3 independent experiments and analysed by one-way ANOVA). (**e**) Change in bead displacement between the first and sixth pulse of force applied to beads coated with anti-nesprin-1 antibody ($n=18$ beads) or anti-NUP358 antibody ($n=16$ beads) and bound to nuclei isolated from HeLa cells. Displacements were calculated relative to the first pulse of force (error bars represent s.e.m., $^*P<0.05$, data were collected from 3 independent experiments and analysed by a two-tailed unpaired $t$-test). Uncropped images of blots are shown in Supplementary Fig. XX.

trichostatin did induce a 2.3-fold increase in the average size of the nuclei. Similar results were obtained when nuclei were treated with DNAse I (Fig. 2b), indicating that chromatin and DNA do not participate in the nuclear adaptation to force. Whereas our results show that DNA does not contribute to nuclear stiffening when mechanical stress is applied on the LINC complex, we cannot exclude that force may affect chromatin organization.

To determine whether the nucleoskeleton mediates the mechanical response of the nucleus to force, we generated stable cell lines depleted for specific nucleoskeletal components using short hairpin RNA (shRNA) (Fig. 2c and Supplementary Fig. 3b) and monitored the change in stiffness of isolated nuclei during pulses of force application. As previously reported by others[12], we observed that depletion of lamin A/C decreased nuclear rigidity (Fig. 2c). Significantly, we found that nuclei isolated from lamin A/C knockdown cells not only exhibited large bead displacements but also failed to stiffen after multiple pulses of force (Fig. 2c). This result shows that lamin A/C is a major determinant of the nuclear strain when mechanical stress is applied on nesprin-1. Thus, strengthening the connection between the LINC complex and lamin A/C could potentially decrease nuclear deformation and contribute to stiffening in response to force on nesprin-1. To test this hypothesis, we isolated the LINC complex in nuclei submitted to force. We found that tension induced the recruitment of lamin A/C, but not lamin B, to the LINC complex in response to force (Fig. 2d), indicating that force on nesprin-1 triggers a reinforcement of the physical connection between lamin A/C and the LINC complex. SUN proteins interact with the KASH domain of nesprins to form the LINC complex and connect nesprins to lamin A/C (refs 2,10,13). To determine whether SUN proteins are required for the nuclear stiffening response, we analysed the mechanical adaptation of nuclei isolated from SUN1 or SUN2 knockdown cells. We found that nuclei depleted of either SUN1 or SUN2 were still able to significantly increase their stiffness following force application, even though they exhibited a decreased stiffening response compared with the control (Fig. 2c). Simultaneous knockdown of both SUN1 and SUN2 completely prevented the nuclear response (Fig. 2c), suggesting that SUN1 and SUN2 both participate in the force response and may have partially redundant roles, as reported by others[14]. Emerin is

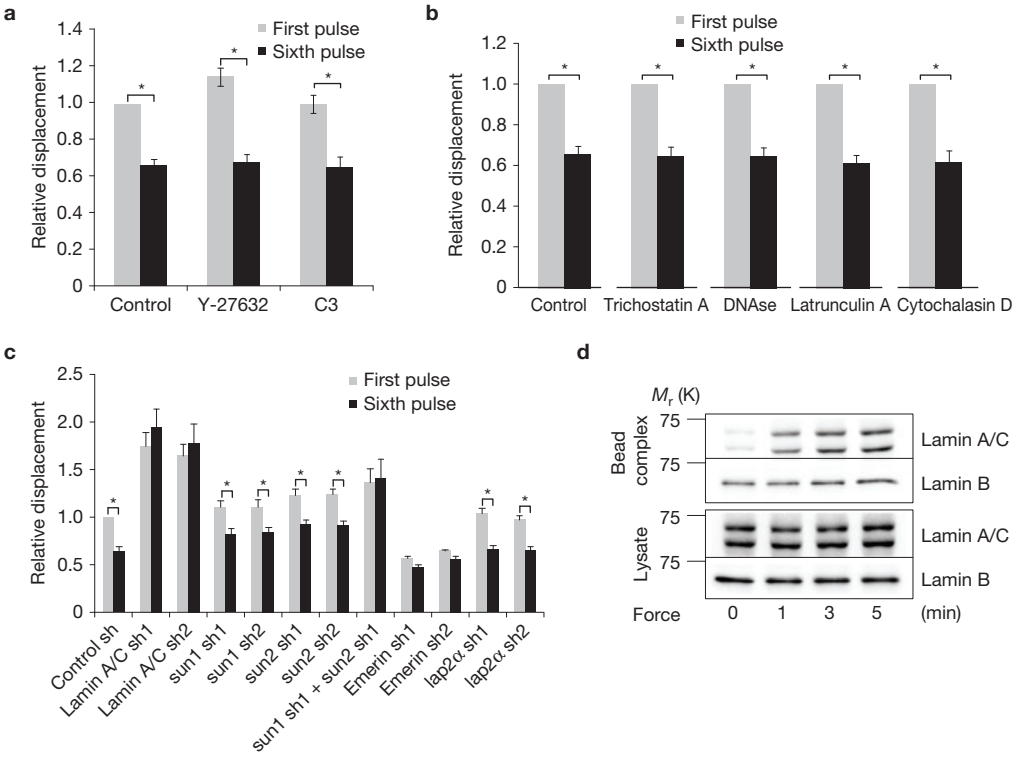


**Figure 2** The nucleoskeleton mediates nuclear stiffening in response to force. (**a**) Change in bead displacement between the first and sixth pulse of force applied to beads coated with anti-nesprin-1 antibody bound to nuclei treated with Y-27632 ($n=17$ beads) or cell-permeable C3 transferase ($n=25$ beads) for 30 min. Displacements were calculated relative to the first pulse of force applied to untreated nuclei (error bars represent s.e.m., $^*P<0.05$, data were collected from 3 independent experiments and analysed by a two-tailed unpaired *t*-test). (**b**) Change in bead displacement between the first and sixth pulse of force applied to beads coated with anti-nesprin-1 antibody bound to nuclei treated with trichostatin A ($n=14$ beads), DNAse1 ($n=16$ beads), latrunculin A (10 μM; $n=19$ beads) or cytochalasin D (5 μM; $n=22$ beads). Displacements were calculated relative to the first pulse of force (error bars represent s.e.m., $^*P<0.05$, data were collected from 3 independent experiments and analysed by a two-tailed unpaired *t*-test). (**c**) Change in bead displacement between the first and sixth pulse of force applied to beads coated with anti-nesprin-1 antibody bound to nuclei isolated from stable cell lines depleted for lamin A/C (sh1 $n=12$ beads; sh2 $n=17$ beads), SUN1 (sh1 $n=19$ beads; sh2 $n=15$ beads), SUN2 (sh1 $n=18$ beads; sh2 $n=14$ beads), SUN1 sh1 + SUN2 sh1 ($n=14$ beads), emerin (sh1 $n=21$ beads; sh2 $n=15$ beads) or LAP2α (sh1 $n=14$ beads; sh2 $n=19$ beads). Displacements were calculated relative to the first pulse of force applied to nuclei isolated from cells expressing control shRNA (error bars represent s.e.m., $^*P<0.05$, data were collected from 3 independent experiments and analysed by a two-tailed unpaired *t*-test). (**d**) Nuclei isolated from HeLa cells were incubated with anti-nesprin-1 coated magnetic beads. After stimulation with a permanent magnet for different amounts of time, the nuclei were lysed with detergent (1% NP-40 in Tris buffer). Then, the protein complexes associated with the beads (bead complex) were isolated from the lysate using a magnetic separation stand and both fractions were denatured, reduced in Laemmli buffer and analysed by western blotting. All results are representative of at least three independent experiments.

a LEM-domain-containing protein of the inner nuclear membrane that binds lamin A/C and whose depletion has been shown to affect nuclear mechanics[15,16]. Interestingly, we found that emerin depletion increased nuclear rigidity and prevented the nuclear adaptation to force (Fig. 2c), whereas depletion of LAP2α (Fig. 2c) or MAN1 (Supplementary Fig. 3c,d), two other LEM-domain proteins, did not affect nuclear stiffening.

Induction of protein phosphorylation is one of the first events that occurs when mechanical force is applied to cells[1,17]. To understand the molecular process that regulates the nuclear adaptation to force, we compared tyrosine phosphorylation of nuclear proteins from isolated nuclei subjected to force or not. We found that force moderately stimulates tyrosine phosphorylation of multiple nuclear proteins (Fig. 3a), but strongly induces tyrosine phosphorylation of a nuclear protein with a relative molecular mass of 35,000 ($M_r$ 35K) that we identified as emerin (Fig. 3a and Supplementary Fig. 4a). Multiple tyrosine kinases have been described in the nucleus, including Src family kinases[18,19] (SFKs), Abl (ref. 20) and FAK (ref. 21). To identify the tyrosine kinase that phosphorylates nuclear proteins in response to force, we used pharmacological inhibitors of SFKs, Abl and FAK and analysed their effects on tyrosine phosphorylation of nuclear proteins induced by applying force on nesprin-1. We found that SFK inhibition (2.5 μM SU66056) prevented force-induced nuclear protein phosphorylation (Supplementary Fig. 4b), including emerin phosphorylation, whereas FAK inhibition (5 μM FAK inhibitor 14) or Abl inhibition (10 μM gleevec) did not affect the increase in tyrosine phosphorylation of nuclear proteins. We also observed that force increased Src phosphorylation on the activation loop tyrosine (Tyr 416; Supplementary Fig. 4c), indicating that force on nesprin-1 activates Src in isolated nuclei. Using proteomic analysis of emerin phosphorylation, a recent study reported that Src specifically phosphorylates emerin at Tyr 59, Tyr 74 and Tyr 95 (ref. 22). We generated shRNA-resistant emerin mutants with tyrosine to phenylalanine substitution for each of these three residues (Y59F, Y74F

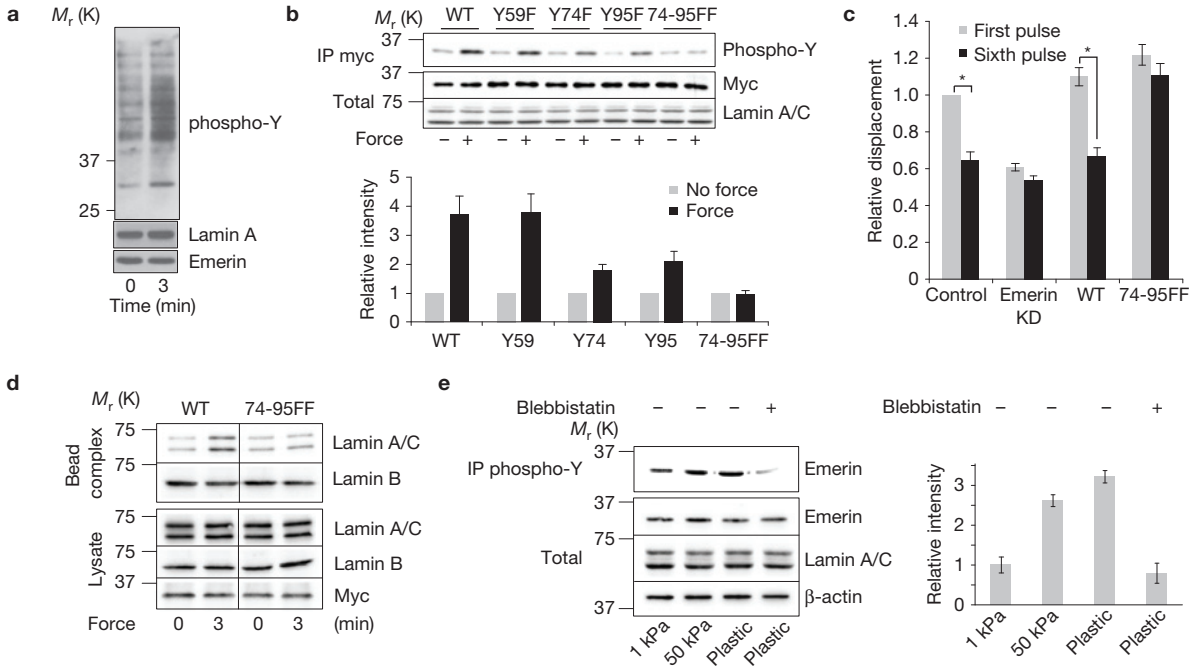


**Figure 3** Emerin phosphorylation on Tyr 74 and Tyr 95 mediates the mechanical adaptation of isolated nuclei to force. (**a**) Nuclei isolated from HeLa cells were incubated with magnetic beads coated with anti-nesprin-1 and stimulated with a permanent magnet for 3 min. Tyrosine phosphorylation of nuclear proteins was analysed by western blotting. All results are representative of at least three independent experiments. (**b**) Nuclei isolated from emerin knockdown HeLa cells re-expressing WT, Y59F, Y74F, Y95F or 74-95FF emerin mutants were incubated with magnetic beads coated with anti-nesprin-1 and stimulated with a permanent magnet for 3 min. Tyrosine phosphorylation of emerin mutants was analysed by western blotting after immunoprecipitation ('total' refers to the emerin level in nuclear lysates). Corresponding densitometric analysis (lower panel) of emerin phosphorylation normalized to emerin levels and expressed as relative to the control in the absence of stimulation by force (error bars represent s.e.m, densitometric data were analysed from $n=4$ independent experiments). (**c**) Change in bead displacement between the first and sixth pulse of force applied to beads coated with anti-nesprin-1 antibody bound to nuclei isolated from emerin knockdown cells re-expressing WT ($n=15$ beads) or 74-95FF emerin mutants ($n=18$ beads). Displacements were calculated relative to the first pulse of force applied to nuclei isolated from emerin knockdown cells (error bars represent s.e.m., $^*P<0.05$, data were collected from 3 independent experiments and analysed by a two-tailed unpaired $t$-test). (**d**) Nuclei isolated from emerin knockdown HeLa cells re-expressing WT or 74-95FF emerin mutants were incubated with magnetic beads coated with anti-nesprin-1 and stimulated with a permanent magnet for 3 min. After stimulation the nuclei were lysed with detergent (1% NP-40 in Tris buffer). Then, the protein complexes associated with the beads (bead complex) were isolated from the lysate using a magnetic separation stand and both fractions were denatured and reduced in Laemmli buffer. All results are representative of at least three independent experiments. (**e**) Emerin tyrosine phosphorylation was analysed after immunoprecipitation in MRC5 cells cultured on matrices with different rigidities (polyacrylamide gels of 1 kPa and 50 kPa and plastic) and treated with blebbistatin. ('Total' refers to the emerin level in nuclear lysates.) Corresponding densitometric analysis (left panel) of emerin phosphorylation normalized to emerin levels and expressed as relative to the 1 kPa condition (error bars represent s.e.m., densitometric data were analysed from $n=4$ independent experiments). Uncropped images of blots are shown in Supplementary Fig. XX.

and Y95F). We then expressed these mutants in emerin knockdown cells and analysed their tyrosine phosphorylation in isolated nuclei subjected to force. We found that application of force on nesprin-1 induced phosphorylation of both wild-type (WT) emerin and the Y59F emerin mutant, whereas mutation of Tyr 74 (Y74F) or to a lesser extent mutation of Tyr 95 (Y95F) decreased emerin phosphorylation in response to force (Fig. 3b). Consistent with these observations, we found no increase in tyrosine phosphorylation of the double mutant (74-95FF) after force application (Fig. 3b). Together these results indicate that force on nesprin-1 activates Src, which, in turn, phosphorylates emerin on Tyr 74 and Tyr 95.

Next, we investigated whether emerin phosphorylation on Tyr 74 and Tyr 95 was necessary for the nuclear adaptation to force. As expected, we found that expression of WT emerin in emerin knockdown cells restored the stiffening of isolated nuclei in response to force (Fig. 3c). In contrast, nuclei expressing the 74-95FF emerin mutant failed to adapt to force (Fig. 3c). In line with this, we did not observe lamin A/C recruitment to the LINC complex in response to force in nuclei expressing the 74-95FF emerin mutant (Fig. 3d) and SFK inhibition prevented the nuclear stiffening in response to force (Supplementary Fig. 4d). Our results show that Src-dependent emerin phosphorylation on Tyr 74 and Tyr 95 mediates the mechanical adaptation of isolated nuclei to force. However, how emerin phosphorylation affects lamin A/C interaction with the LINC complex remains to be elucidated. Interestingly, SUN2 and emerin interact with the same part of lamin A/C (ref. 23), suggesting that they may compete for binding to lamin A/C and force-induced emerin phosphorylation may potentially affect SUN2 interaction with lamin A/C and reinforce the connection between nesprin and the nucleoskeleton. Nesprin-1 binds actin filaments and transmits both externally applied force and cell-generated force to the nucleoskeleton. To investigate whether emerin phosphorylation is regulated by cell-generated contractility, we analysed emerin phosphorylation during cell adhesion to fibronectin. Emerin phosphorylation increased during

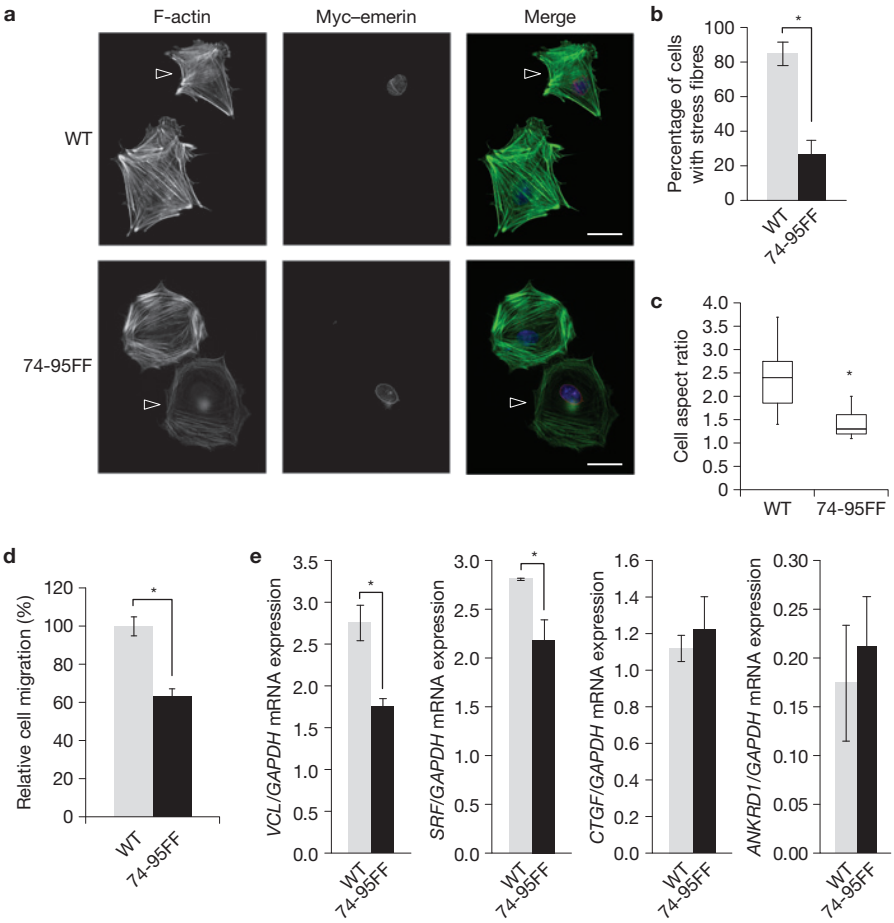


**Figure 4** Emerin phosphorylation on Tyr 74 and Tyr 95 affects stress fibre formation and SRF-dependent gene expression. (**a**) Emerin knockdown MRC5 cells re-expressing WT or the 74-95FF emerin mutant (arrowhead) were grown on fibronectin-coated coverslips, fixed, permeabilized and stained for F-actin (Alexa488–phalloidin) and myc-tagged emerin. Scale bars, 25 μm. All results are representative of 4 independent experiments. (**b**) Cells were treated as above and analysed for stress fibres. The graph represents the mean of $n = 64$ myc-positive cells expressing WT emerin and $n = 67$ myc-positive cells expressing 74-95FF. Data were analysed by a blinded observer (error bars represent s.e.m., $^*P < 0.05$, data were collected from 4 independent experiments and analysed by a two-tailed unpaired *t*-test). (**c**) Cells were treated as above and the cell aspect ratio analysed. A number of $n = 64$ myc-positive cells expressing WT emerin and $n = 67$ myc-positive cells expressing 74-95FF were analysed. Box plots indicate median values and capture 50% of data in boxes and 75% between the lines ($^*P < 0.05$, data were collected from 4 independent experiments and analysed by a two-tailed unpaired *t*-test). (**d**) Invasion of emerin knockdown HeLa cells re-expressing WT or 74-95FF emerin mutant was evaluated by Transwell migration assays. Cells were plated in the upper chamber of the filters and after 8 h cells that had migrated to the underside of the filters were fixed. Relative cell migration was determined by the number of cells that had migrated to the underside of the filter normalized to the total number of cells. A number of $n = 24$ fields were observed per condition. The value from control shRNA HeLa cells was arbitrarily set at 100% (error bars represent s.e.m, $^*P < 0.05$ compared with WT data were collected from 4 independent experiments and analysed by one way ANOVA). (**e**) *VCL*, *SRF*, *CTGF*, *ANKRD1* and *GAPDH* mRNA levels were analysed by real-time qPCR in emerin knockdown MRC5 cells re-expressing WT or the 74-95FF emerin mutant. Results are expressed as relative mRNA expression levels (error bars represent s.e.m., $^*P < 0.05$, data were collected from $n = 4$ independent experiments and analysed by a two-tailed unpaired *t*-test).

adhesion and this increase was blocked by inhibiting actomyosin contractility with blebbistatin (Supplementary Fig. 5a). Substrate rigidity regulates cell contractility; cells on rigid substrates have been shown to exhibit greater contractility than cells plated on soft substrates[24]. We observed that fibroblasts grown on rigid substrates have increased emerin phosphorylation (Fig. 3e). We also found that application of tensional force on integrin, using fibronectin-coated beads, increased emerin phosphorylation (Supplementary Fig. 5b). These results demonstrate that emerin phosphorylation is regulated by cell-generated contractility and externally applied force, and indicate that emerin regulates nuclear rigidity in response to mechanical cues experienced by the whole cell.

LINC complex components interact with perinuclear actin filaments[25,26] and it has been reported that disruption of the LINC complex or depletion of lamin A/C affects the organization of the actin cytoskeleton[23,27,28], presumably because a subset of actin filaments require attachment at the nuclear surface. As emerin phosphorylation on Tyr 74 and Tyr 95 regulates the magnitude of strain when tension is applied on the LINC complex, we reasoned that emerin phosphorylation may be important for anchoring actin filaments to the LINC complex. We found that emerin-deficient fibroblasts that expressed the phosphoresistant emerin mutant (74-95FF) exhibited less bundled actin filaments (Fig. 4a,b). This indicates that nuclear adaptation to force is critical for actin cytoskeletal

organization, reinforcing the idea that structural elements are physically interdependent in cells, as proposed previously[2,3]. Impaired connection of the actin cytoskeleton with the nucleus has been shown to affect polarization and motility[23]. Remarkably, expression of phosphoresistant emerin 74-95FF resulted in defects in polarization and migration through pores (Fig. 4c,d).

We next analysed the effect of emerin phosphorylation on mechanosensitive gene expression. Using real-time quantitative PCR (qPCR), we first examined serum response factor (SRF)-dependent transcription. We found that expression of phosphoresistant emerin (74-95FF) decreased expression of *VCL* (vinculin) and *SRF* (Fig. 4e). The transcription regulators YAP and TAZ have been recently described as sensors and mediators of mechanical cues. We observed that emerin-deficient fibroblasts that expressed the 74-95FF emerin mutant exhibited less nuclear localization of YAP and TAZ (Supplementary Fig. 5d). However, we detected no effect on connective tissue growth factor (*CTGF*) and ankyrin repeat domain 1 (*ANKRD1*) messenger RNA levels (Fig. 4e), two YAP/TAZ-regulated genes. Emerin deficiency has been shown to impact *IEX1* expression in response to strain[15]; interestingly, we found that expression of the 74-95FF emerin mutant decreased the *IEX1* basal level but it did not prevent *IEX1* induction by tensional force application (Supplementary Fig. 5e). Our results are consistent with recent findings that emerin regulates megakaryoblastic leukaemia 1 (MKL1, also known as MAL or MRTF) nuclear localization and SRF-dependent transcription[29]. This previous work indicated that emerin regulates MKL1 signalling by controlling polymerization of nuclear actin[29]. Whereas we found that nuclear actin did not contribute to the nuclear stiffening observed in response to force (Fig. 2b), this previous work raises the possibility that emerin phosphorylation regulates nuclear mechanics and transcription through potentially different pathways.

Nuclear mechanics affect many features of cell behaviour including motility[28,30], polarity and cell survival[23]. Previous work showed that nuclear rigidity can be modulated during differentiation[11] or in response to long-term application of shear stress on cells[31]. Here we show that isolated nuclei are able to adjust their rigidity within seconds in response to tension, suggesting that nuclei adapt their mechanical properties to the stress they experience, whether it is externally applied to the cell or generated in the cell itself. Our finding that isolated nuclei produce a mechanical response to force suggests that other organelles may similarly contribute to the integrated cellular mechanoresponse. Mechanical stress transmission to the nucleus depends on many factors, including cytoskeletal pre-stress, LINC complex structure and nucleoskeleton organization. All of these elements are known to vary substantially between cell types[2,11,23], possibly reflecting the need for the nuclei of these cells to respond differently to mechanical cues. Future work will help to determine in which physiological or pathological contexts nuclear mechanotransduction pathways are regulated.

## METHODS

Methods and any associated references are available in the online version of the paper.

*Note: Supplementary Information is available in the online version of the paper*


### ACKNOWLEDGEMENTS

This study was supported by National Institutes of Health Grants numbers GM029860 (to K.B.), P41-EB002025-23A1 (R.S.) and R01-HL077546-03A2 (R.S.), and a grant from the University Cancer Research Fund from the Lineberger Comprehensive Cancer Center. C.G. is supported by a Marie Curie Outgoing International Fellowship from the European Union Seventh Framework Programme (FP7/2007-2013) under grant agreement no 254747.


### AUTHOR CONTRIBUTIONS

C.G. designed and performed experiments. L.S., L.D.O., L.V.L., R.S. and R.G-M. helped with experimental design and procedures. C.G. and K.B. wrote the manuscript. K.B. directed the project. All authors provided detailed comments.

### COMPETING FINANCIAL INTERESTS

The authors declare no competing financial interests.


Published online at www.nature.com/doifinder/10.1038/ncb2927
Reprints and permissions information is available online at www.nature.com/reprints



1. Hoffman, B. D., Grashoff, C. & Schwartz, M. A. Dynamic molecular processes mediate cellular mechanotransduction. *Nature* **475,** 316–323 (2011).
2. Wang, N., Tytell, J. D. & Ingber, D. E. Mechanotransduction at a distance: Mechanically coupling the extracellular matrix with the nucleus. *Nat. Rev. Mol. Cell Biol.* **10,** 75–82 (2009).
3. Maniotis, A. J., Chen, C. S. & Ingber, D. E. Demonstration of mechanical connections between integrins, cytoskeletal filaments, and nucleoplasm that stabilize nuclear structure. *Proc. Natl Acad. Sci. USA* **94,** 849–854 (1997).
4. Wang, N., Butler, J. P. & Ingber, D. E. Mechanotransduction across the cell surface and through the cytoskeleton. *Science* **260,** 1124–1127 (1993).
5. Matthews, B. D., Overby, D. R., Mannix, R. & Ingber, D. E. Cellular adaptation to mechanical stress: Role of integrins, Rho, cytoskeletal tension and mechanosensitive ion channels. *J. Cell Sci.* **119,** 508–518 (2006).
6. Choquet, D., Felsenfeld, D. P. & Sheetz, M. P. Extracellular matrix rigidity causes strengthening of integrin-cytoskeleton linkages. *Cell* **88,** 39–48 (1997).
7. Guilluy, C. *et al.* The Rho GEFs LARG and GEF-H1 regulate the mechanical response to force on integrins. *Nat. Cell Biol.* **13,** 724–729 (2011).
8. Hofmann, W. A. & de Lanerolle, P. Nuclear actin: To polymerize or not to polymerize. *J. Cell Biol.* **172,** 495–496 (2006).
9. Dubash, A. D. *et al.* The small GTPase RhoA localizes to the nucleus and is activated by Net1 and DNA damage signals. *PloS ONE* **6,** e17380 (2011).
10. Dahl, K. N. & Kalinowski, A. Nucleoskeleton mechanics at a glance. *J. Cell Sci.* **124,** 675–678 (2011).
11. Pajerowski, J. D., Dahl, K. N., Zhong, F. L., Sammak, P. J. & Discher, D. E. Physical plasticity of the nucleus in stem cell differentiation. *Proc. Natl Acad. Sci. USA* **104,** 15619–15624 (2007).
12. Lammerding, J. *et al.* Lamin A/C deficiency causes defective nuclear mechanics and mechanotransduction. *J. Clin. Invest.* **113,** 370–378 (2004).
13. Sosa, B. A., Rothballer, A., Kutay, U. & Schwartz, T. U. LINC complexes form by binding of three KASH peptides to domain interfaces of trimeric SUN proteins. *Cell* **149,** 1035–1047 (2012).
14. Lei, K. *et al.* SUN1 and SUN2 play critical but partially redundant roles in anchoring nuclei in skeletal muscle cells in mice. *Proc. Natl Acad. Sci. USA* **106,** 10207–10212 (2009).
15. Lammerding, J. *et al.* Abnormal nuclear shape and impaired mechanotransduction in emerin-deficient cells. *J. Cell Biol.* **170,** 781–791 (2005).
16. Rowat, A. C., Lammerding, J. & Ipsen, J. H. Mechanical properties of the cell nucleus and the effect of emerin deficiency. *Biophys. J.* **91,** 4649–4664 (2006).
17. Sawada, Y. *et al.* Force sensing by mechanical extension of the Src family kinase substrate p130Cas. *Cell* **127,** 1015–1026 (2006).
18. Takahashi, A. *et al.* Nuclear localization of Src-family tyrosine kinases is required for growth factor-induced euchromatinization. *Exp. Cell Res.* **315,** 1117–1141 (2009).
19. Chu, I. *et al.* p27 phosphorylation by Src regulates inhibition of cyclin E-Cdk2. *Cell* **128,** 281–294 (2007).
20. Taagepera, S. *et al.* Nuclear-cytoplasmic shuttling of C-ABL tyrosine kinase. *Proc. Natl Acad. Sci. USA* **95,** 7457–7462 (1998).
21. Lim, S. T. *et al.* Nuclear FAK promotes cell proliferation and survival through FERM-enhanced p53 degradation. *Mol. Cell* **29,** 9–22 (2008).
22. Tifft, K. E., Bradbury, K. A. & Wilson, K. L. Tyrosine phosphorylation of nuclear-membrane protein emerin by Src, Abl and other kinases. *J. Cell Sci.* **122,** 3780–3790 (2009).
23. Ho, C. Y. & Lammerding, J. Lamins at a glance. *J. Cell Sci.* **125,** 2087–2093 (2012).
24. Provenzano, P. P. & Keely, P. J. Mechanical signaling through the cytoskeleton regulates cell proliferation by coordinated focal adhesion and Rho GTPase signaling. *J. Cell Sci.* **124,** 1195–1205 (2011).
25. Khatau, S. B. *et al.* A perinuclear actin cap regulates nuclear shape. *Proc. Natl Acad. Sci. USA* **106,** 19017–19022 (2009).
26. Luxton, G. W., Gomes, E. R., Folker, E. S., Vintinner, E. & Gundersen, G. G. Linear arrays of nuclear envelope proteins harness retrograde actin flow for nuclear movement. *Science* **329,** 956–959 (2010).

27. Folker, E. S., Ostlund, C., Luxton, G. W., Worman, H. J. & Gundersen, G. G. Lamin A variants that cause striated muscle disease are defective in anchoring transmembrane actin-associated nuclear lines for nuclear movement. *Proc. Natl Acad. Sci. USA* **108,** 131–136 (2011).
28. Khatau, S. B. *et al.* The distinct roles of the nucleus and nucleus-cytoskeleton connections in three-dimensional cell migration. *Sci. Rep.* **2,** 488 (2012).
29. Ho, C. Y., Jaalouk, D. E., Vartiainen, M. K. & Lammerding, J. Lamin A/C and emerin regulate MKL1-SRF activity by modulating actin dynamics. *Nature* **497,** 507–511 (2013).
30. Friedl, P., Wolf, K. & Lammerding, J. Nuclear mechanics during cell migration. *Curr. Opin. Cell Biol.* **23,** 55–64 (2011).
31. Philip, J. T. & Dahl, K. N. Nuclear mechanotransduction: Response of the lamina to extracellular stress with implications in aging. *J. Biomechanics* **41,** 3164–3170 (2008).

DOI: 10.1038/ncb2927

## METHODS

**Cell lines, reagents and antibodies.** HeLa and MRC5 cells were grown in Dulbecco's modified Eagle's medium (DMEM; Invitrogen) supplemented with 10% fetal bovine serum (Sigma) and antibiotic–antimycotic solution (Sigma). HUVECs were grown in endothelial cell growth medium (Lonza). Hydrogels with different stiffness were purchased from Matrigen and coated with fibronectin (50 μg ml$^{-1}$ for 45 min). Latrunculin A was purchased from Tocris Bioscience, cytochalasin D was from Calbiochem and DNAse I was from Pierce. Cell-permeable C3 transferase was from Cytoskeleton. Trichostatin A and poly-L-Lysine (0.01% solution $M_r$ 75K–150K) were from Sigma. FAK inhibitor 14 was purchased from Tocris Bioscience and used at 5 μM. SU6656 was from EMD Millipore and used at 2.5 μM. Gleevec was purchased from Novartis and used at 10 μM. Antibodies against LBR (ab32535, 1:750), MAN1 (9E1, 1:1,000), nesprin-1 (ab24742—immunogen: recombinant fusion protein corresponding to amino acids 1–428 of recombinantly expressed rat nesprin-1-α) and LAP2 (ab11823, 1:2,000) were from Abcam, anti phosphotyrosine antibody (PY20, 1:1,000) and anti SUN2 (1:750) were purchased from Millipore, anti-myc (9E10.3, 1:250 for immunofluorescence and 1:1,000 for western blot) was from Invitrogen, anti-emerin (4G5, 1:1,000) was from Neomarkers and anti-SUN1 (1:500) was purchased from Sigma. Anti Nup358 was from Thermoscientific. Anti-YAP/TAZ (1:250) was purchased from Cell Signaling. Anti-lamin A/C (H-110, 1:1,000) and anti-lamin B (M-20, 1:1,000) were from Santa Cruz.

**cDNA and shRNA.** pCMV6-Entry mouse emerin (carboxy-terminal myc and DDK tagged) was purchased from Origene (MR222146). Tyrosine to phenylalanine substitutions of Tyr 59, Tyr 74 and Tyr 95 were performed using site-directed mutagenesis according to the QuikChange site-directed mutagenesis kit instruction manual (Stratagene). Lentiviral shRNA targeting human emerin, LAP2, SUN1, SUN2, lamin A/C and lentiviral non-targeting control vector were purchased from Open Biosystems. Emerin sh1(Oligo ID: TRCN0000083011) hairpin sequence: 5′-CCGGCGACTACTATGAAGAGAGCTACTCGAGTAGCTCTCTTCATAGTAG TCGTTTTTG-3′; emerin sh2 (Oligo ID: TRCN0000083011) hairpin sequence: 5′-CCGGCAGGTGCATGATGACGATCTTCTCGAGAAGATCGTCATCATGCACC TGTTTTTG-3′; lamin A/C sh1 (Oligo ID TRCN0000061837) hairpin sequence: 5′-CCGGGCCGTGCTTCCTCTCACTCATCTCGAGATGAGTGAGAGGAAGCA CGGCTTTTTG-3′; lamin A/C sh2 (Oligo ID TRCN0000061836) hairpin sequence: 5′-CCGGCATGGGCAATTGGCAGATCAACTCGAGTTGATCTGCCAATTGCC CATGTTTTTG-3′; SUN1 sh1 (Oligo ID TRCN0000133901) hairpin sequence: 5′-CCGGCAGATACACTGCATCATCTTTCTCGAGAAAGATGATGCAGTGTATC TGTTTTTTG-3′; SUN1 sh2 (Oligo ID TRCN0000135899) hairpin sequence: 5′-CCGGGAACTAGAACAGACCAAGCAACTCGAGTTGCTTGGTCTGTTCTAG TTCTTTTTTG-3′; SUN2 sh1 (Oligo ID TRCN0000143335) hairpin sequence: 5′-CCGGGCCTATTCAGACGTTTCACTTCTCGAGAAGTGAAACGTCTGAAT AGGCTTTTTTG-3′; SUN2 sh2 (Oligo ID TRCN0000141958) hairpin sequence: 5′-CCGGGCAAGACTCAGAAGACCTCTTCTCGAGAAGAGGTCTTCTGAGTCT TGCTTTTTTG-3′; LAP2α sh1 (Oligo ID TRCN0000116482) hairpin sequence: 5′-CCGGCAGGTACTTTATGCCAACATTCTCGAGAATGTTGGCATAAAGTACC TGTTTTTG-3′; LAP2α sh2 (Oligo ID TRCN0000116484) hairpin sequence: 5′-CCGGGCACAGATTCTTAGCTCAGATCTCGAGATCTGAGCTAAGAATCTGT GCTTTTTG-3′.

**Nucleus isolation.** HeLa cells were plated (48 h, 70% confluence) on 150 mm dishes and serum starved for 16 h. After one wash with PBS (room temperature, 10 ml), cells were lysed with 6 ml of hypotonic buffer (10 mM HEPES, 1 mM KCl, 1.5 mM $MgCl_2$, 0.5 mM dithiothreitol, and protease inhibitors) and cell bodies were detached using a cell scraper (Sarstedt). After incubating for 5 min on ice, samples were homogenized using 30 strokes of a tight-fitting Dounce homogenizer and centrifuged at 700*g* for 5 min at 4 °C. Pellets were washed in hyponic buffer and centrifuged again. Then, the nuclear pellet was suspended in buffer S (20 mM HEPES at pH 7.8, 25 mM KCl, 5 mM $MgCl_2$, 0.25 M sucrose and 1 mM ATP). For force microscopy experiments, 10,000 nuclei were plated on a poly-L-lysine-coated coverslip for 30 min at 37 °C in 0.5 ml of buffer I (20 mM HEPES at pH 7.8, 25 mM KCl, 5 mM $MgCl_2$ and 1 mM ATP). For biochemistry, $10^6$ nuclei were plated on poly-L-lysine-coated dishes (35 mm) for 30 min at 37 °C in 1 ml I buffer. Then, nuclei were incubated with magnetic beads coated with anti-nesprin-1 (2.8 μm Invitrogen) at 37 °C for 20 min. After two washes with buffer I, the nuclei were incubated in buffer S (20 mM HEPES at pH 7.8, 25 mM KCl, 5 mM $MgCl_2$, 0.25 M sucrose and 1 mM ATP) for 15 min at 37 °C. Isolated nuclei were then stimulated with force using the permanent magnet for different amounts of time.

**Magnetic tweezers.** The UNC three-dimensional force microscope[32] was used for applying controlled and precise 15–35 pN local force on the magnetic beads. Nuclei were plated on poly-L-lysine-coated coverslips for 30 min and incubated for 20 min after addition of beads. On force application, bead displacements were recorded with a high-speed video camera (Rolera EM-C2—Qimaging) and tracked using Video Spot Tracker (Center for Computer Integrated Systems for microscopy and manipulation, http://cismm.cs.unc.edu). The UNC three-dimensional force microscope system was calibrated before experiments using a fluid of known viscosity. Displacement of individual beads attached to nuclei was tracked using Video Spot Tracker software. Only beads located on top of the nuclei were selected for analysis to prevent substrate contributions. Beads that showed displacements of less than 10 nm (detection resolution—Supplementary Table 1) and loosely bound beads were not selected for analysis. Spring constants were calculated as previously described[33] (details in Supplementary Fig. 2).

**Permanent magnet system calibration.** The permanent magnet assays were conducted using a 1.25-inch-diameter × 0.25-inch-thick nickel-plated neodymium (grade N52) magnet (K&J Magnetics) suspended 4.5 mm over nuclei plated on a 35-mm-diameter culture dish. Using finite element analysis software (COMSOL Multiphysics 4.3), the magnetic force experienced by the nuclei (incubated with 2.8 μm magnetic beads) due to the permanent magnet was calculated to be between 20 and 25 pN.

**Immunoprecipitation.** Cells were lysed directly in hot gel sample buffer (100 mM Tris at pH 6.8, 10% glycerol, 2% SDS and 2.5% 2-ME), boiled for 10 min and sonicated. Samples were then diluted with 20 volumes of 1% Triton X-100 and 1% DOC in Tris-buffered saline (TBS). After preclearing (20 min), a total of 2 μg of PY-20 monoclonal anti-phospho-tyrosine antibody (or 2 μg of anti emerin antibody) was incubated with the samples for 2 h at 4 °C. Then, protein G–Sepharose (Millipore) beads were added and incubated for 45 min at 4 °C and samples were then washed five times in 1% Triton X-100 and 1% DOC in TBS, and analysed by western blotting.

**LINC complex isolation after force application.** Nuclei isolated from HeLa cells were incubated with magnetic beads coated with anti-nesprin-1. After stimulation with a permanent magnet for different amounts of time, the nuclei were lysed with detergent (20 mM Tris at pH 7.6, 150 mM NaCl, 1% NP-40, 2 mM $MgCl_2$, and protease inhibitors) and with sonication. Then, the protein complex associated with the beads (bead complex) was isolated from the lysate using a magnetic separation stand and both fractions were denatured and reduced in Laemmli buffer.

**Purification of recombinant proteins.** Construction of the pGEX4T-1 prokaryotic expression constructs containing Rho-binding domain (RBD) of rhotekin have been described previously[34]. Briefly, expression of the fusion proteins in *Escherichia coli* was induced with 100 M isopropyl-β-D-thiogalactoside (IPTG) for 16 h at room temperature. Bacterial cells were lysed in buffer containing 50 mM Tris at pH 7.6, 150 mM NaCl, 5 mM $MgCl_2$, 1 mM dithiothreitol, 10 μg ml$^{-1}$ each of aprotinin and leupeptin, and 1 mM phenylmethyl sulphonyl fluoride, and the proteins were purified by incubation with glutathione–Sepharose 4B beads (GE Healthcare) at 4 °C.

**GST–RBD pulldowns.** Active RhoA-pulldown experiments were carried out as described elsewhere[33]. Isolated nuclei were lysed in 50 mM Tris (pH 7.6), 500 mM NaCl, 1% Triton X-100, 0.1% SDS, 0.5% deoxycholate, 10 mM $MgCl_2$, 200 μM orthovanadate, and protease inhibitors. After removal of the magnetic beads using the magnetic separator (Invitrogen), lysates were clarified by centrifugation at 13,000*g*, equalized for total volume and protein concentration, and rotated for 30 min with 30 μg of purified GST–RBD bound to glutathione–Sepharose beads. The bead pellets were washed in 50 mM Tris (pH 7.6), 150 mM NaCl, 1% Triton X-100, 10 mM $MgCl_2$, 200 μM orthovanadate, and protease inhibitors, and subsequently processed for SDS–PAGE.

**Immunofluorescence.** Cells were fixed for 15 min in 4% formaldehyde, permeabilized in 0.2% Triton X-100 for 10 min, and blocked for 10 minutes in 1% BSA. Immunofluorescence images were taken with a Zeiss Axiovert 200M microscope equipped with a Hamamatsu ORCA-ERAG digital camera and Metamorph workstation (Universal Imaging). To quantify stress fibres, myc-positive cells were scored by a blinded observer for the presence or absence of stress fibres; the criteria were: organized, thickened parallel actin bundles throughout most of the cytoplasm. Cell aspect ratio was calculated as the ratio of the long axis to the short axis of the best-fit ellipse for each cell. To quantify YAP or TAZ nuclear localization, we calculated the percentage of cells with a predominant nuclear staining (delimited by DAPI staining) among the total cell number.

**Invasion assay.** Collected HeLa cells were fluorescently labelled using CellTracker (Invitrogen) and plated onto the upper chamber of a Transwell filter with 8 μm pores (Corning). The upper chamber was placed in serum-free DMEM and the lower chamber contained 10% serum in DMEM. After 8 h, cells were fixed with 4%

paraformaldehyde in PBS. Non-migrated cells on the upper side of the filter were removed with a cotton swab.

**qPCR with reverse transcription.** Total RNA was purified from cells using the RNAqueous-Micro kit (Ambion-Life technologies) according to the manufacturer's instructions. RNA (0.8 µg) was reverse-transcribed into cDNA using the High Capacity cDNA Reverse Transcription kit (Applied Biosystems). Quantitative real-time PCR was conducted on a StepOnePlus using TaqMan Master Mix (Applied Biosystems) and TaqMan primers/probes for *IEX-1* (IER3; (Hs04187506_g1), *SRF* (Hs00182371_m1), *VCL* (Hs00419715_m1), *CTGF* (Hs01026927_g1) and *ANKRD1* (Hs00173317_m1) according to the manufacturer's recommendations. Expression data were normalized to a standard curve generated from a pool of control cells. *GAPDH* (glyceraldehyde-3-phosphate dehydrogenase; Hs02786624_g1) was used as the reference gene. Data are based on results from four independent experiments (for Fig. 4e) and three independent experiments (for Supplementary Fig. 5f). Three technical replicates were performed in each independent experiment.

**Statistics.** Statistical analyses were performed using Sigma Stat (GraphPad Software). Data are presented as mean ± s.e.m. unless stated otherwise. A two-tailed unpaired *t*-test and one-way ANOVA were used as detailed in respective figure legends. Statistical significance was defined as $P < 0.05$. All representative images were observed in at least three independent experiments (Figs 1a, 2d, 3a,b,d,e and Fig. 4a and Supplementary Figs 3a,b,d, 4a–c and 5a,b,d). Exclusion criteria were used for the analysis of the magnetic tweezers data and are described in the Methods above (Magnetic tweezers section). These exclusion criteria were pre-established before performing the quantification. Randomization was not used in the entire study. For Fig. 4b, data were analysed by a blinded observer. For all other studies in the manuscript, the investigators were not blinded to allocation during experiments and outcome assessment. The numbers of independent experiments performed for all of the quantitative data are indicated in the figure legends.

32. Fisher, J. K. *et al.* Thin-foil magnetic force system for high-numerical-aperture microscopy. *Rev. Sci. Instrum.* **77,** nihms8302 (2006).
33. Guilluy, C. *et al.* The Rho GEFs LARG and GEF-H1 regulate the mechanical response to force on integrins. *Nat. Cell Biol.* **13,** 724–729 (2011).
34. Ren, X. D., Kiosses, W. B. & Schwartz, M. A. Regulation of the small GTP-binding protein Rho by cell adhesion and the cytoskeleton. *EMBO J.* **18,** 578–585 (1999).

**Queries for NPG paper ncb2927**

**Page 1**

*Query 1:*
Please note that the title has been changed according to style.

**Page 1**

*Query 2:*
'via' changed to 'through' here. OK?

**Page 2**

*Query 3:*
Please check sentence 'Uncropped images...' added to the end of the caption of figures 1 and 3, and provide Supplementary Figure number.

**Page 2**

*Query 4:*
Is 'Although' better than 'Whereas' here, and in the sentence 'Whereas it has' in the first (bold) paragraph?

**Page 3**

*Query 5:*
In figure 2c, should 'sun' and 'lap' be 'SUN' and 'LAP' throughout? Also, please check the use of 'Nup' versus 'NUP' throughout the text and figures.

**Page 3**

*Query 6:*
Text amended to 'of a nuclear ... ($M_r$ 35K)' here (and a similar change made in the Methods). Please check.

**Page 3**

*Query 7:*
'while' changed to 'whereas' here, to avoid non-time-related uses of the former. OK?

**Page 6**

*Query 8:*
Please check the use of 'Whereas' here.

**Page 7**

*Query 9:*
Please provide page range for ref. 28.

**Page 8**

*Query 10:*
Text written as '(ab24742—immunogen: recombinant'here. OK?

**Page 8**

*Query 11:*
Text written as 'isopropyl-β-D-thiogalactoside' here. OK?

**Page 9**

*Query 12:*
Heading written as 'qPCR with reverse transcription'. OK?